Defective Lipolysis and Altered Energy Metabolism in Mice Lacking Adipose Triglyceride Lipase

Guenter Haemmerle *et al.*

Science **312**, 734 (2006);
DOI: 10.1126/science.1123965

Science (print ISSN 0036-8075; online ISSN 1095-9203) is published weekly, except the last week in December, by the American Association for the Advancement of Science, 1200 New York Avenue NW, Washington, DC 20005.

20. T. D. Ford, *Proc. Yorks. Geol. Soc.* **31**, 211 (1958).
21. B. N. Runnegar, *Neues Jahrb. Geol. Paläontol. Abh.* **195**, 303 (1995).
22. S. Conway Morris, *Palaeontology* **36**, 593 (1993).
23. J. Dzik, *J. Morphol.* **252**, 315 (2002).
24. S. Jensen, J. G. Gehling, M. L. Droser, *Nature* **393**, 567 (1998).
25. J. W. Hagadorn, C. M. Fedo, B. M. Waggoner, *J. Paleontol.* **74**, 731 (2000).
26. W.-T. Zhang, L. Babcock, *Acta Palaeontol. Sinica* **40** (Suppl.), 201 (2001).
27. The phylogenetic questions associated with Ediacaran taxa have largely precluded a higher-level taxonomy. This ordinal designation would include both the taxon described here and such genera as *Charniodiscus*, *Glaessnerina*, *Khatyspytia*, *Vaizitsinia*, and possibly *Charnia*.
28. M. Medina, A. G. Collins, J. D. Silberman, M. L. Sogin, *Proc. Natl. Acad. Sci. U.S.A.* **98**, 9707 (2001).
29. A. Ender, B. Schierwater, *Mol. Biol. Evol.* **20**, 130 (2003).
30. T. Hadrys, R. DeSalle, S. Sagasser, N. Fischer, B. Schierwater, *Mol. Biol. Evol.* **22**, 1569 (2005).
31. M. Podar, S. H. D. Haddock, M. L. Sogin, G. R. Harbison, *Mol. Phyl. Evol.* **21**, 218 (2001).
32. A. G. Collins *et al.*, *Syst. Biol.* **55**, 97 (2006).
33. K. J. Peterson, M. McPeek, D. A. D. Evans, *Paleobiology* **2** (Suppl.), 36 (2005).
34. We thank Y. Ji, M. Cheng, and J. Zhai at the Early Life Institute; S. Last, S. Capon, and V. Brown at Cambridge for technical assistance; and N. Butterfield and three anonymous referees for critical remarks. The work is supported by the National Natural Science Foundation of China, Ministry of Science and Technology of China, Program for Changjiang Scholars and Innovative Research Team in University (PCSIRT), the Cowper-Reed Fund, and St. John's College, Cambridge.

Supporting Online Material
www.sciencemag.org/cgi/content/full/312/5774/731/DC1
Figs. S1 and S2

4 January 2006; accepted 31 March 2006
10.1126/science.1124565

Defective Lipolysis and Altered Energy Metabolism in Mice Lacking Adipose Triglyceride Lipase

Guenter Haemmerle,[1] Achim Lass,[1] Robert Zimmermann,[1] Gregor Gorkiewicz,[2] Carola Meyer,[5] Jan Rozman,[5] Gerhard Heldmaier,[5] Robert Maier,[3] Christian Theussl,[6] Sandra Eder,[1] Dagmar Kratky,[4] Erwin F. Wagner,[6] Martin Klingenspor,[5] Gerald Hoefler,[2] Rudolf Zechner[1]*

Fat tissue is the most important energy depot in vertebrates. The release of free fatty acids (FFAs) from stored fat requires the enzymatic activity of lipases. We showed that genetic inactivation of adipose triglyceride lipase (ATGL) in mice increases adipose mass and leads to triacylglycerol deposition in multiple tissues. ATGL-deficient mice accumulated large amounts of lipid in the heart, causing cardiac dysfunction and premature death. Defective cold adaptation indicated that the enzyme provides FFAs to fuel thermogenesis. The reduced availability of ATGL-derived FFAs leads to increased glucose use, increased glucose tolerance, and increased insulin sensitivity. These results indicate that ATGL is rate limiting in the catabolism of cellular fat depots and plays an important role in energy homeostasis.

Adipose tissue mass in mammals is determined by the dynamic equilibrium of lipid synthesis and lipid catabolism. Disruptions of this balance underlie metabolic diseases such as obesity and type II diabetes (*1*–*3*). Hormone-sensitive lipase (HSL) was once thought to be the major enzyme responsible for the lipolytic breakdown of cellular fat stores (*4*–*6*). However, HSL-deficient mice are lean, and they efficiently mobilize FFAs from triacylglycerol (TG) stores (*7*, *8*), suggesting that other TG hydrolases play an important role. Recently, we and others reported the discovery of an enzyme that we named in accordance with its physiological activity: adipose triglyceride lipase (ATGL) (*9*–*11*). Other designations for this enzyme have been: transport secretion protein (TTS), desnutrin (*10*), calcium-independent phospholipase A2z (iPL-A2z) (*11*), adiposome triglyceride lipase (ATGL) (*12*), and patatin-like phospholipase domain–containing protein 2 (PNPLP2). ATGL specifically hydrolyses long-chain fatty acid TG (*9*, *11*) and is predominantly expressed in adipose tissue and, to a lesser extent, in cardiac muscle, skeletal muscle, testis tissue, and other tissues. The finding that ATGL mRNA expression is regulated by fasting/feeding (*10*) as well as hormones and cytokines (*13*, *14*), and that the inhibition of ATGL in vitro (*9*, *12*) markedly decreases TG catabolism, imply that the enzyme plays an important role in lipolysis.

To elucidate the physiological function of ATGL during lipid mobilization in vivo, we inactivated the *Atgl* gene in mice by replacing the first exon, including the translational start codon and the lipase consensus sequence motif (GXSXG, where G is Gly, S is Ser, and X is any amino acid), with a neomycin expression cassette (fig. S1). *Atgl*(−/−) mice showed accumulation of neutral lipid to supraphysiological levels in most tissues, suggesting an essential role for ATGL in cellular TG catabolism (table S1). The TG content in tissues of *Atgl*(+/−) mice resembled that of wild-type (WT) mice, except for cardiac muscle where there was a twofold increase. Compared with WT mice, *Atgl*(−/−) animals were heavier (Fig. 1A and fig. S2A), displayed a twofold increase in whole body fat mass, and exhibited enlarged adipose fat depots (Fig. 1B and fig. S2, B and C). The mutants had an increased wet weight of gonadal (2.1-fold) and inguinal white adipose tissue (WAT) (1.6-fold), as well as intrascapular brown adipose tissue (BAT) (8.5-fold). Ad libitum food intake [3.6 ± 0.6 g in *Atgl*(−/−) mice and 3.3 ± 0.7 g in WT mice] and lean body mass (Fig. 1A) were similar in mice of both genotypes. Consistent with increased adipose weight, plasma leptin levels were elevated in fed (2.1-fold) and fasted (4.4-fold) *Atgl*(−/−) mice (table S2). The leptin/fat mass ratio, however, was similar in mutant and control mice. Morphological analyses of adipose tissue from *Atgl*(−/−) mice (fig. S2C) revealed enlarged lipid droplets in white [4690 ± 235 μm^2 for *Atgl*(−/−) versus 3382 ± 90 μm^2 for WT] and brown adipocytes [1395 ± 119 μm^2 for *Atgl*(−/−) versus 67 ± 10 μm^2 for WT; n = 100 cells analyzed, $P < 0.001$]. The multilocular lipid droplets normally observed in BAT became unilocular and strongly resembled white fat in appearance. Thus, the absence of ATGL in mice causes fat cell hypertrophy and mild obesity.

In cardiac muscle, ATGL deficiency caused severe TG accumulation (Fig. 1, C and E). At the age of 12 weeks, mice had a TG content in myocytes more than 20 times higher in *Atgl*(−/−) mice than in WT controls, causing a 1.4-fold increase in heart weight [193 ± 18 mg for *Atgl*(−/−) versus 131 ± 12 mg for WT, $P < 0.001$, $n = 8$]. Histological analyses revealed an age-dependent increase of lipid droplets in number and size in cardiomyocytes, starting with microvesicular lipid accumulation at the age of 6 weeks and progressing to the accumulation of large droplets at the age of 18 weeks (Fig. 1E). This massive lipid buildup led to severe cardiac insufficiency. In echocardiography (Fig. 1E and table S3), the ejection fraction of the left ventricle was drastically reduced in *Atgl*(−/−) mice (40.2 ± 26.5%) compared with WT (80.5 ± 17.1%, $P < 0.001$). Additionally, a marked disturbance of cardiac texture and increased fibrosis was noted (Fig. 1E). The interventricular septum (1.9 ± 0.6 mm)

[1]Institute of Molecular Biosciences, University of Graz, Austria. [2]Institute of Pathology; [3]Department of Cardiology; [4]Institute of Molecular Biology and Biochemistry, Center of Molecular Medicine, Medical University of Graz, Austria. [5]Department of Animal Physiology, Faculty of Biology, Philipps-University Marburg, Germany. [6]Research Institute of Molecular Pathology, Vienna, Austria.

*To whom correspondence should be addressed. E-mail: rudolf.zechner@uni-graz.at

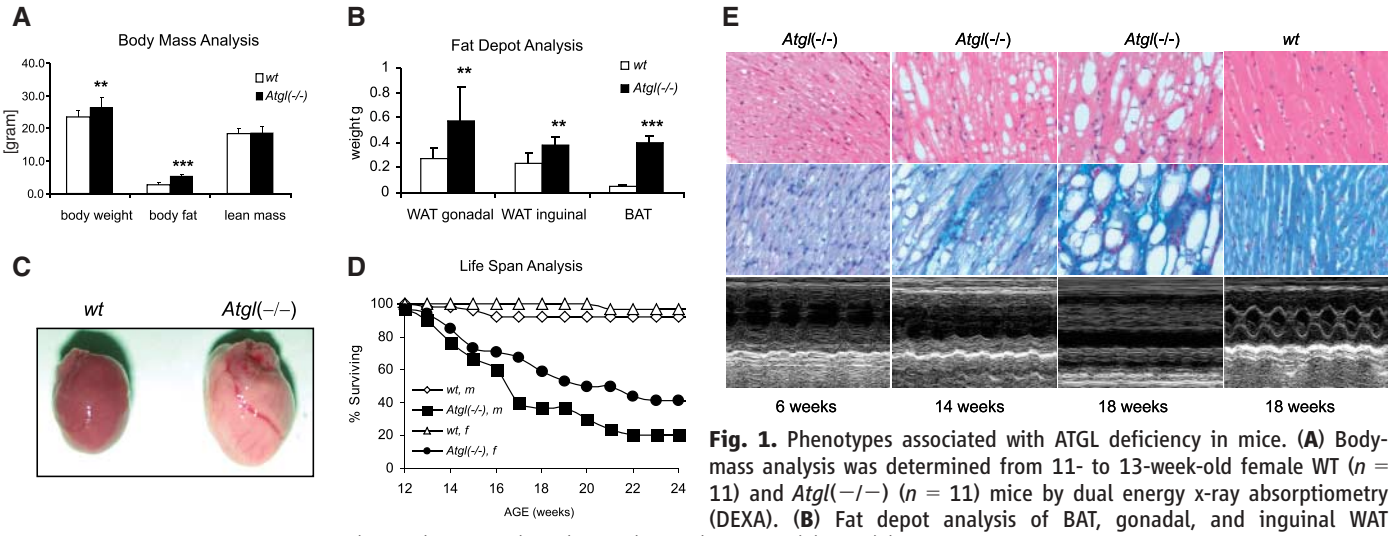

Fig. 1. Phenotypes associated with ATGL deficiency in mice. (**A**) Body-mass analysis was determined from 11- to 13-week-old female WT (n = 11) and *Atgl*(−/−) (n = 11) mice by dual energy x-ray absorptiometry (DEXA). (**B**) Fat depot analysis of BAT, gonadal, and inguinal WAT dissected from 14- to 16-week-old WT (n = 12) and *Atgl*(−/−) mice (n = 11). Data in (A) and (B) are shown as mean ± SD. Statistical significance was determined by a two-tailed Student's t-test comparing WT and *Atgl*(−/−) mice (**P < 0.01, ***P < 0.001). (**C**) Photographs of hearts from 14-week-old WT and *Atgl*(−/−) mice. Note the yellow discoloration due to lipid accumulation in the heart of *Atgl*(−/−) mice. (**D**) Kaplan-Meier plot showing the cumulative survival of WT (m, males n = 53; f, females n = 33) and *Atgl*(−/−) mice, (males n = 30, females n = 34) over a period of 24 weeks. (**E**) Heart histology and echocardiographic analysis. *Atgl*(−/−) mice show progressing triglyceride accumulation in cardiomyocytes (hematoxilin/eosin stain, top row) and myocardial fibrosis indicated by fiber specific staining (chromotrope aniline blue stain, dark blue, middle row) increasing with age. WT animals show none of these alterations (right column). Echocardiography of *Atgl*(−/−) mice revealed increasing concentric left-ventricular hypertrophy and impairment of left-ventricular systolic function (M-mode imaging, bottom row).

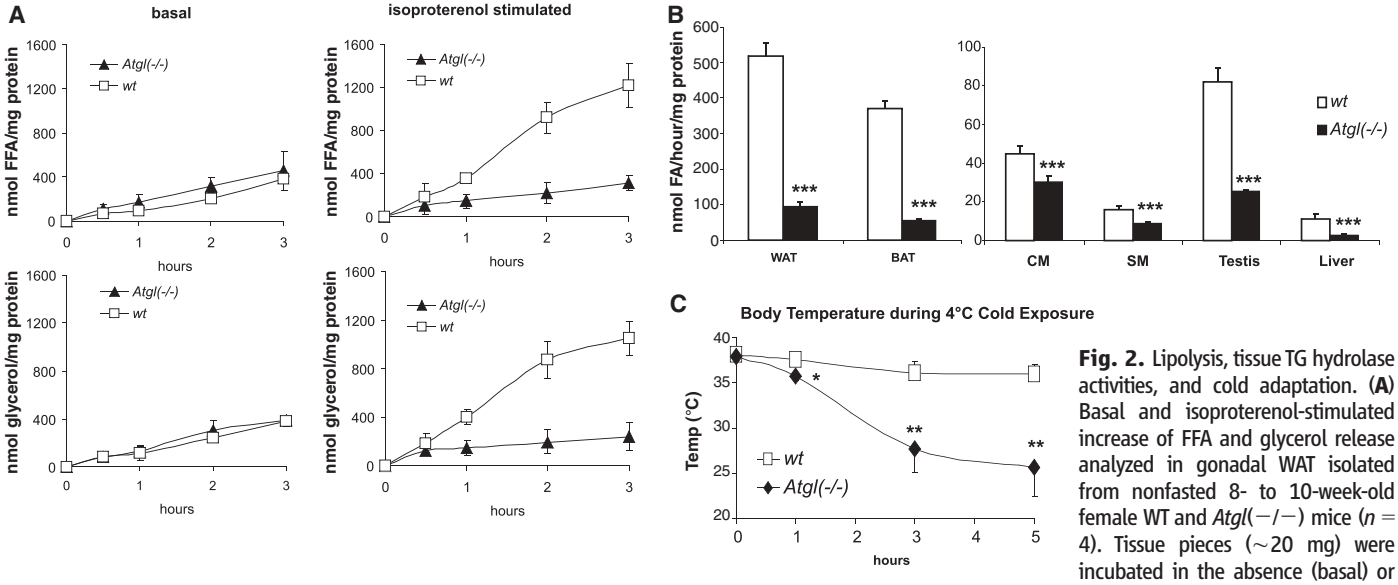

Fig. 2. Lipolysis, tissue TG hydrolase activities, and cold adaptation. (**A**) Basal and isoproterenol-stimulated increase of FFA and glycerol release analyzed in gonadal WAT isolated from nonfasted 8- to 10-week-old female WT and *Atgl*(−/−) mice (n = 4). Tissue pieces (~20 mg) were incubated in the absence (basal) or presence of 10 μM isoproterenol (isoproterenol-stimulated). Isoproterenol-mediated increase was calculated by the subtraction of basal values. **(B)** TG-hydrolase activities were determined in cytosolic fractions of tissues from fasted 10- to 12-week-old female WT and *Atgl*(−/−) mice (n = 5). CM, cardiac muscle; SM, skeletal muscle; (**C**) Body temperature of 11- to 12-week-old male WT and *Atgl*(−/−) mice was determined during exposure to 4°C for 5 hours. Three mice were used for each time point and genotype. All data are shown as mean ± SD (*P < 0.05, **P < 0.01, ***P < 0.001).

and the posterior wall of the left ventricle (1.8 ± 0.6 mm) were significantly thicker in *Atgl*(−/−) hearts than in controls (1.2 ± 0.2 mm, P < 0.005, and 1.2 ± 0.4 mm, P < 0.05, respectively) and increased with age. Consistent with tissue damage, a moderate (less than 1% of cells) induction of apoptosis was noted in *Atgl*(−/−) mice by caspase 3 immunohistochemistry (fig. S3A). Signs of inflammation were not detected. The pronounced cardiac dysfunction resulted in premature death of male and female *Atgl*(−/−) mice. As shown in the Kaplan-Meier plot (Fig. 1D), the first *Atgl*(−/−) mice died around 12 weeks after birth. Male mice died earlier (50% after 16 weeks) than females (50% after 20 weeks). In contrast, male and female *Atgl*(+/−) mice had a normal life expectancy. At dissection, deceased *Atgl*(−/−) mice exhibited typical features of congestive heart failure. These included marked dilatation of both left and right ventricles, congestion of pulmonary blood vessels and edema (fig. S3), pleural as well as cardiac effusions (fig. S4), and extensive blood congestion of organs (fig. S3). None of these features were present in control animals or *Atgl*(−/−) mice analyzed morphologically before the age of 14 weeks.

Table 1. Comparison of plasma parameters in WT mice, heterozygous [*Atgl*(+/−)], and homozygous ATGL-deficient [*Atgl*(−/−)] mice. Plasma lipids, glucose, insulin, and metabolites were measured in fed or fasted (overnight fast) female 10- to 12-week-old mice. Essentially similar data were observed for male *Atgl*(−/−) mice. FFA, free fatty acids; TG, triacylglycerols; KB, ketone bodies; TC, total cholesterol. Data are shown as mean ± SD from at least six mice per genotype and measurement condition. Mean values of each plasma component are compared between WT and *Atgl*(−/−) mice and WT and *Atgl*(+/−) mice, respectively. Statistical significance was determined by a two-tailed Student's *t*-test (**P* < 0.05, ***P* < 0.01, ****P* < 0.001). n.d., not determined.

	WT		*Atgl*(+/−)		*Atgl*(−/−)	
	Fed	Fasted	Fed	Fasted	Fed	Fasted
FFA (mmol/L)	0.40 ± 0.07	0.79 ± 0.32	0.37 ± 0.14	0.93 ± 0.35	0.28 ± 0.05*	0.30 ± 0.08**
TG (mg/dl)	81.5 ± 14.7	60.5 ± 19.6	84.7 ± 28.5	48.6 ± 15.6	79.8 ± 13.6	20.2 ± 8.0**
KB (mmol/L)	n.d.	2.09 ± 0.30	n.d.	1.72 ± 0.37	n.d.	0.60 ± 0.25***
TC (mg/dl)	105.8 ± 21.1	91.9 ± 10.5	94.1 ± 12.6	95.1 ± 6.0	98.1 ± 19.0	71.5 ± 12.1*
Glucose (mg/dl)	142.1 ± 8.6	82.2 ± 10.8	140.6 ± 9.5	81.6 ± 5.1	136.6 ± 16.4	78.6 ± 11.8
Insulin (ng/ml)	0.82 ± 0.28	0.20 ± 0.06	0.93 ± 0.46	0.24 ± 0.11	0.48 ± 0.21*	0.25 ± 0.11

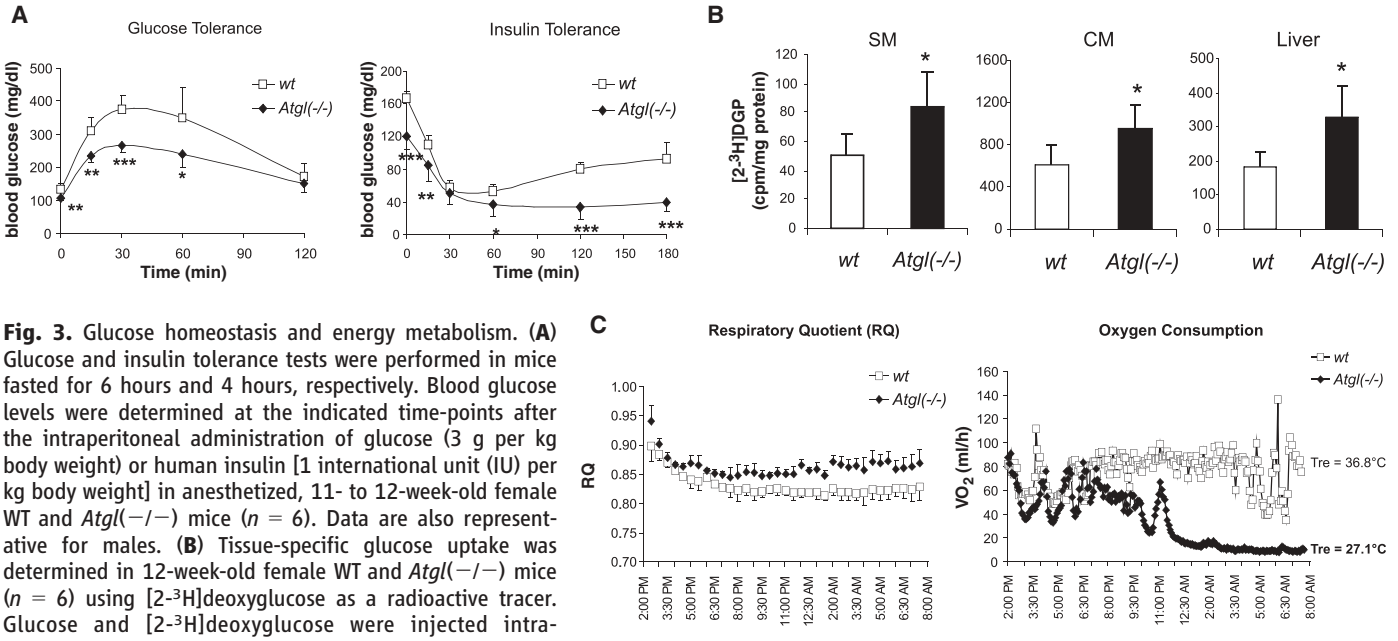

Fig. 3. Glucose homeostasis and energy metabolism. (**A**) Glucose and insulin tolerance tests were performed in mice fasted for 6 hours and 4 hours, respectively. Blood glucose levels were determined at the indicated time-points after the intraperitoneal administration of glucose (3 g per kg body weight) or human insulin [1 international unit (IU) per kg body weight] in anesthetized, 11- to 12-week-old female WT and *Atgl*(−/−) mice (n = 6). Data are also representative for males. (**B**) Tissue-specific glucose uptake was determined in 12-week-old female WT and *Atgl*(−/−) mice (n = 6) using [2-^{3}H]deoxyglucose as a radioactive tracer. Glucose and [2-^{3}H]deoxyglucose were injected intraperitoneally under the conditions described for the glucose tolerance test, and the accumulation of [2-^{3}H]deoxyglucose-6-phosphate ([2-^{3}H]DGP) was determined in skeletal muscle (SM), cardiac muscle (CM), and the liver. (**C**) Time course of the RQ and oxygen consumption (VO_2) in 12- to 13-week-old female WT and *Atgl*(−/−) mice (n = 8) during 18 hours of food deprivation at 24°C. Mean RQ ± SD values were significantly lower in WT mice than in *Atgl*(−/−) mice ($P < 0.01$) after 3 hours of food removal. VO_2 (measured every 5 min) was significantly decreased in *Atgl*(−/−) mice compared with WT mice ($P < 0.01$) after 5 hours of food removal. A representative plot for one *Atgl*(−/−) and one WT mouse is shown for VO_2. Hypometabolism is also reflected by decreased rectal temperature (T_{re}) in *Atgl*(−/−) mice mesasured immediately after removal of the mice from the metabolic cage. Data are shown as mean ± SD. Statistical significance was determined in a two-tailed Student's *t*-test (for glucose measurements) or by analysis of variance (ANOVA) (RQ and VO_2 analysis) (**P* < 0.05, ***P* < 0.01, ****P* < 0.001).

Thus, the functional, histological, and pathological observations indicate that *Atgl*(−/−) mice die from cardiac insufficiency caused by a mechanical contraction defect resulting from the massive accumulation of lipids.

In other nonadipose tissues, the most pronounced accumulation of TG (>10-fold) occurred in the testis and kidney (table S1), although smaller increases in fat content (1.5- to 4-fold) were observed in essentially all tissues, including the liver. Thus, an important lipolytic function of ATGL is generally implied for nonadipose tissues. TG deposition in the kidney was not associated with lipiduria or increased plasma creatinine or urea levels in *Atgl*(−/−) mice, indicating normal renal function.

To identify the biochemical defect caused by ATGL-deficiency, we analyzed the β-adrenergic stimulated lipolytic capacity of normal and ATGL-deficient WAT. Explants of gonadal white fat were incubated in the presence or absence of isoproterenol, and the release of FFAs and glycerol was determined hourly. As shown in Fig. 2A, the basal release of FFAs and glycerol from *Atgl*(−/−) WAT was similar to that from WT tissue. In contrast, isoproterenol-stimulated lipolysis was drastically reduced in *Atgl*(−/−) WAT. After a 2-hour incubation period, 74% fewer FFAs and 78% less glycerol were released from mutant versus WT WAT. Similarly, the TG hydrolase activity in *Atgl*(−/−) WAT and BAT was decreased by 82% and 85%, respectively (Fig. 2B). Lipolytic activities were also reduced in cardiac muscle (–31%), skeletal muscle (–44%), the testis (–69%), and the liver (–73%) of *Atgl*(−/−) mice. Thus, alternative lipases such as HSL or triglyceride hydrolase (TGH) (*15*) cannot efficiently compensate for the absence of ATGL in adipose and other peripheral tissues. These results also support the hypothesis that HSL might be more important as a diacylglycerol hydrolase than as a TG hydrolase (*9*, *16*).

Impaired catabolism of TG in BAT caused a severe defect in thermoregulation in *Atgl*(−/−) mice. Upon cold exposure for 5 hours, *Atgl*(−/−) mice suffered from life-threatening hypothermia (body temperature, 25°C) (Fig. 2C). This phenotype resembles that of β-adrenergic receptor–deficient mice (*17*) and suggests that in the absence of ATGL, insufficient amounts of FFAs are released as energy substrate for uncoupled mitochondrial respiration. Consistent with the observed defect in adaptive thermogenesis, peroxisome proliferator activated receptor-γ coactivator-1α (PGC-1α) and uncoupling protein-1 (UCP-1) expression were decreased by 80% and 53% in *Atgl*(−/−) mice compared with WT mice, respectively (fig. S5). Thus, HSL cannot compensate for the defective lipolysis in BAT of *Atgl*(−/−) mice. In contrast, HSL-deficient mice expressing normal amounts of ATGL are not cold sensitive (*7*), indicating that ATGL provides adequate amounts of FFAs for thermogenesis. Additionally, both male and female *Atgl*(−/−) mice are fertile, whereas HSL-deficient male mice are sterile (*18*).

Table 1 summarizes measurements of plasma lipid metabolism and carbohydrate metabolism in *Atgl*(−/−), *Atgl*(+/−), and WT mice. Coherent with the observed defective lipolysis in WAT, *Atgl*(−/−) mice exhibited reduced plasma FFA concentrations in both the fed and in the fasted state (–30 and –62%, respectively). Plasma concentrations for TG (–66%), β-hydroxy-butyrate (–71%), and total cholesterol (–22%) were also lower in fasted *Atgl*(−/−) mice. The decrease in plasma TG and cholesterol concentrations in *Atgl*(−/−) mice was due to reduced plasma very low–density lipoprotein (VLDL) and high-density lipoprotein levels (HDL), respectively (fig. S6). Reduced FFA, TG, VLDL, and β-hydroxy-butyrate levels were also reported for HSL-deficient mice (*19*) and might result from lower transport rates of FFAs to the liver in both animal models, leading to decreased hepatic VLDL synthesis and ketogenesis (*19*). In contrast with HSL-deficient mice exhibiting increased HDL-cholesterol levels, *Atgl*(−/−) animals had reduced plasma concentrations of HDL cholesterol.

A reciprocal relationship exists between the use of FFAs and glucose as substrates for energy production (*20*). Elevated uptake, storage, and oxidation of FFAs in muscle is associated with increased insulin resistance, resulting in increased plasma glucose and insulin levels (*21*–*23*). This adverse effect of FFAs in nonadipose tissues is commonly referred to as "lipotoxicity" (*24*, *25*). According to the view that FFAs and acyl–coenzyme A (CoA) derivatives, and not fat per se, exert "lipotoxic" effects (*26*, *27*), the reduced release of FFAs from stored fat in adipose tissue and (cardiac) muscle of ATGL-deficient mice should promote "antilipotoxic" effects, such as decreased FFA oxidation, increased glucose use, and increased glucose tolerance. Consistent with this hypothesis, in fed *Atgl*(−/−) mice, plasma insulin levels were reduced by 42%, whereas plasma glucose concentrations were similar to those in WT animals (Table 1). No significant changes in glucose or insulin levels were observed in heterozygous *Atgl*(+/−) mice when compared with control animals. In the fasted state (overnight fast), insulin and glucose concentrations were similar in mice of all three genotypes. In glucose tolerance tests (Fig. 3A), 6-hour fasted *Atgl*(−/−) mice exhibited significantly lower basal glucose values and displayed a markedly improved glucose tolerance compared with WT mice. In insulin tolerance tests (Fig. 3A), the maximal decline of blood glucose levels was more pronounced in *Atgl*(−/−) mice (34 mg/dl) than in WT mice (53 mg/dl) and persisted over the whole measurement period of 3 hours. In WT mice, a rebound of glucose values occured after 60 min. Glucose uptake experiments revealed that the accumulation of 2-deoxyglucose was markedly elevated in skeletal muscle (68%), cardiac muscle (54%), and in the liver (78%) (Fig. 3B) of *Atgl*(−/−) mice. Thus, glucose uptake and insulin sensitivity/resistance may be determined by the capacity of ATGL to mobilize FFA.

Consistent with increased glucose uptake and utilization, the respiratory quotient (RQ) of *Atgl*(−/−) mice deviated from that of WT during fasting (Fig. 3C). During ad libitum feeding and the first 2 hours of fasting, RQ values were similar in *Atgl*(−/−) and WT mice. With increasing fasting time, the RQ in WT mice decreased further, which is indicative of increased lipid oxidation, whereas the RQ in *Atgl*(−/−) mice remained at a constant elevated level. Simultaneously, a gradual decrease in oxygen consumption indicating reduced energy expenditure was observed in *Atgl*(−/−) mice (Fig. 3C). After 18 hours of fasting, oxygen consumption was only 25% of that found in control mice. Furthermore, the body temperature dropped to 28.4 ± 2.2°C in *Atgl*(−/−) mice, compared with 35.4 ± 1.8°C in WT mice in response to prolonged fasting.

Our studies suggest that in mice, ATGL is the rate-limiting enzyme for the initiation of TG catabolism in adipose and many nonadipose tissues. The association of ATGL deficiency with increased glucose tolerance, increased insulin sensitivity, and increased RQ during fasting provides compelling evidence that the decreased availability of FFAs promotes the use of glucose as metabolic fuel despite the presence of massive amounts of fat in adipose tissue and muscle. The inability to mobilize these fat stores leads to energy starvation, resulting in reduced energy expenditure, a decline in body temperature, and premature death when *Atgl*(−/−) animals are stressed by cold exposure or food deprivation. Thus, ATGL plays a crucial role in energy homeostasis in mice. The observations that ATGL contributes to adipocyte lipolysis in human adipose tissue (*28*) and that genetic variation in the human *ATGL* gene is associated with plasma FFA, TG, and type II diabetes (*29*) suggest that our findings in mice may also be relevant for human physiology.

References and Notes

1. B. B. Kahn, J. S. Flier, *J. Clin. Invest.* **106**, 473 (2000).
2. B. M. Spiegelman, J. S. Flier, *Cell* **104**, 531 (2001).
3. G. I. Shulman, *J. Clin. Invest.* **106**, 171 (2000).
4. D. M. Raben, J. J. Baldassare, *Trends Endocrinol. Metab.* **16**, 35 (2005).
5. H. Mulder *et al.*, *Diabetes* **48**, 228 (1999).
6. V. Large *et al.*, *J. Lipid Res.* **39**, 1688 (1998).
7. J. Osuga *et al.*, *Proc. Natl. Acad. Sci. U.S.A.* **97**, 787 (2000).
8. G. Haemmerle *et al.*, *J. Biol. Chem.* **277**, 4806 (2002).
9. R. Zimmermann *et al.*, *Science* **306**, 1383 (2004).
10. J. A. Villena, S. Roy, E. Sarkadi-Nagy, K. H. Kim, H. S. Sul, *J. Biol. Chem.* **279**, 47066 (2004).
11. C. M. Jenkins *et al.*, *J. Biol. Chem.* **279**, 48968 (2004).
12. E. Smirnova *et al.*, *EMBO Rep.* **7**, 106 (2006).
13. S. Kralisch *et al.*, *Mol. Cell. Endocrinol.* **240**, 43 (2005).
14. E. E. Kershaw *et al.*, *Diabetes* **55**, 148 (2006).
15. K. G. Soni *et al.*, *J. Biol. Chem.* **279**, 40683 (2004).
16. G. Haemmerle *et al.*, *J. Biol. Chem.* **277**, 4806 (2002).
17. E. S. Bachman *et al.*, *Science* **297**, 843 (2002).
18. J. Osuga *et al.*, *Proc. Natl. Acad. Sci. U.S.A.* **97**, 787 (2000).
19. G. Haemmerle *et al.*, *J. Biol. Chem.* **277**, 12946 (2002).
20. P. J. Randle, P. B. Garland, C. N. Hales, E. A. Newsholme, *Lancet* **1**, 785 (1963).
21. J. D. McGarry, R. L. Dobbins, *Diabetologia* **42**, 128 (1999).
22. M. Roden *et al.*, *J. Clin. Invest.* **97**, 2859 (1996).
23. G. Boden, X. Chen, J. Ruiz, J. V. White, L. Rossetti, *J. Clin. Invest.* **93**, 2438 (1994).
24. Y. T. Zhou *et al.*, *Proc. Natl. Acad. Sci. U.S.A.* **97**, 1784 (2000).
25. R. H. Unger, *Annu. Rev. Med.* **53**, 319 (2002).
26. L. L. Listenberger *et al.*, *Proc. Natl. Acad. Sci. U.S.A.* **100**, 3077 (2003).
27. H. C. Chiu *et al.*, *J. Clin. Invest.* **107**, 813 (2001).
28. D. Langin *et al.*, *Diabetes* **54**, 3190 (2005).
29. V. Schoenborn *et al.*, *Diabetes,* in press.

30. We thank H. Braunias, A. Haumer, A. Hermann, B. Juritsch, H. Reicher, C. Schober, R. Schreiber, and G. Szerencsi for administrative and technical assistance; Siemens Medical Solutions for providing the echo machine and transducer; and E. Zechner for critically reviewing the manuscript. Supported by the Austrian Fonds zur Förderung der Wissenschaftlichen Forschung (SFB-Biomembranes F00701 and F00713) and the Austrian Federal Ministry of Education, Science, and Culture (GEN-AU project Genomics of Lipid-associated Disorders–GOLD), and the NGFN2 Neuronet Obesity and Related Disorders (FKZ01GS0483).

Supporting Online Material

www.sciencemag.org/cgi/content/full/312/5774/734/DC1
Materials and Methods
SOM Text
Figs. S1 to S6
Tables S1 to S3
References

16 December 2005; accepted 5 April 2006
10.1126/science.1123965